Absence of pure voltage instabilities in the third-order model of power grid dynamics

Cite as: Chaos **32**, 043105 (2022); doi: 10.1063/5.0080284
Submitted: 30 November 2021 · Accepted: 16 March 2022 ·
Published Online: 4 April 2022

View Online Export Citation CrossMark

Moritz Thümler,[1,a)] Xiaozhu Zhang,[1,b)] and Marc Timme[1,2]

AFFILIATIONS

[1]Chair for Network Dynamics, Institute for Theoretical Physics and Center for Advancing Electronics Dresden (cfaed), Technische Universität Dresden, 01069 Dresden, Germany
[2]Lakeside Labs, Lakeside B04b, Klagenfurt 9020, Austria

[a)]**Author to whom correspondence should be addressed:** moritz.thuemler@tu-dresden.de
[b)]**Present address:** MOE Key Laboratory of Advanced Micro-Structured Materials and School of Physics Science and Engineering, Tongji University, Shanghai 200092, P. R. China and Frontiers Science Center for Intelligent Autonomous Systems, Tongji University, Shanghai 200092, P. R. China

ABSTRACT

Secure operation of electric power grids fundamentally relies on their dynamical stability properties. For the third-order model, a paradigmatic model that captures voltage dynamics, three routes to instability are established in the literature: a pure rotor angle instability, a pure voltage instability, and one instability induced by the interplay of both. Here, we demonstrate that one of these routes, the pure voltage instability, requires infinite voltage amplitudes and is, thus, nonphysical. We show that voltage collapse dynamics nevertheless exist in the absence of any voltage instabilities.

Most aspects of our daily life essentially depend on a reliable supply of electrical power, thereby imposing severe challenges for the stable operation of power grids that consist of many generators (producers of electric power) and loads (consumers of power) connected with transmission lines. From a perspective of network dynamical systems, these challenges translate to requiring steady states that are (asymptotically) stable against sufficiently small dynamical perturbations such that all dynamical variables relax back to their steady synchronous (phase-locked) state with fixed phase differences and constant overall grid frequency, as well as fixed voltage amplitudes. In contrast, instabilities may cause growth or fluctuations of phase differences, deviating and changing frequencies, and non-constant voltage levels, all undesired in power grid operation. For the most basic model class of power system dynamics that covers voltage dynamics, three routes to instabilities have been established in the literature. Here, we demonstrate that only two of these three remain in the physically relevant regime, while the third is physically excluded as it is inconsistent with finite and positive voltage amplitudes.

I. INTRODUCTION

Electric power supply substantially relies on the stable power grid dynamics. Two classes of system variables are especially important for reliable grid operation: grid frequency and terminal voltage amplitudes.[1–3] Instabilities to fluctuations and collapse of terminal voltages have been identified as key contributing factors for large-scale blackouts, for instance, in the northeastern United States (2003) and Athens/Greece (2004).[2,3] The phenomena of voltage collapse and voltage instability in power system models have been extensively studied in the literature (see, e.g., Refs. 4–6).

Since more than a decade ago, beginning with the derivation of a dynamic network model from the physics of coupled synchronous machines[7] and its collective dynamical phenomena such as phase-locking and synchronization in larger networks,[8] the self-organized nonlinear dynamics of entire power grid networks have drawn vast attention among research communities. The collective dynamics of such systems were studied regarding global asymptotic stability,[6–9] real-world statistical properties of fluctuations,[10,11] and induced response dynamics[12] up to dynamically induced cascading failures.[13,14] All such works have contributed to a conceptual understanding of the stability properties and, in particular, various types of instabilities in power grid dynamics on the system's level. In one of the most fundamental dynamic models, a power grid network consists of nodes that are synchronous machines modeling electrical motors or generators. A range of models of this class with various degrees of detail have been studied in the literature.[2,15] A most commonly studied model consists of coupled swing equations, employing the *second order model* of synchronous machines.[7] Here, the independent variables describing the state of each machine i are given by the deviation of the power angle $\Theta_i(t)$ from an operating point and its time derivative $\dot{\Theta}_i(t)$ quantifying the local deviation from the grid frequency, with a nominal value of $2\pi \times 50\,\mathrm{Hz}$ in Europe and $2\pi \times 60\,\mathrm{Hz}$ in the United States.[16] Grid frequency constitutes an important quantity for grid operators to control the dynamical state of power grids.[1,2] The second order model of synchronous machines takes the terminal voltage amplitudes E_i to be constant and, therefore, cannot address any instabilities resulting from the dynamics of voltages. The *third-order model* constitutes the next higher-order model and enables a dynamical description of terminal voltage amplitudes.[2,6,9] In particular, three routes to instability are established in the literature[6,9] for the third-order model: one pure rotor angle instability, one pure voltage instability, as well as an instability related to the interplay of rotor angle and voltage dynamics. In this work, we differentiate between linear (asymptotic) stability of the voltage subsystem, known as the pure voltage instability in the literature, and alterations of voltage variables upon parameter changes that are not related to a change of the linear stability of the voltage subsystem. We refer to the first one as *voltage instability* or instability of the voltage subsystem and the latter as *voltage collapse*.

In this article, we demonstrate that the pure voltage instability in the third-order model is inconsistent with finite voltage amplitudes and thus physically impossible. It emerges as an artifact of extending the parameter regime of the model to a regime where at least one machine is practically disconnected from the transmission system. Employing Gershgorin's circle theorem, we analytically show that the relevant eigenvalues of the local Jacobian stay negative and bounded away from zero if all voltage amplitudes are kept finite and positive. Thus, instabilities of the voltage subsystem are not captured by the third-order model in the regime that is physically relevant. Moreover, we numerically demonstrate that voltage collapse is still observable in the third-order model within the physically relevant parameter regime if active power demand cannot be met due to limitations in the dynamic transmission capacities.

II. NECESSARY CONDITIONS FOR PURE VOLTAGE INSTABILITIES IN THE THIRD-ORDER MODEL

The loss of acceptable voltage levels has been observed in different forms in real-world power systems.[1] Mathematical models of power systems predict the existence of both, voltage collapse, and instabilities and capture transitions from normal operation to dysfunctional states by bifurcations induced by varying parameters across specific critical values.[15]

Let us consider the third-order model, a dynamical systems model of a power grid that consists of N generators and consumers modeled as synchronous machines, which are interconnected by alternating current (AC) transmission lines. The third-order model captures three dynamical variables per node i, a phase angle $\Theta_i(t)$, its instantaneous rotation frequency $\omega_i(t) = d\Theta_i/dt(t)$ and a voltage amplitude $E_i(t)$. The dynamics of one synchronous machine i reads[2,6]

$$\begin{aligned} \dot{\Theta}_i &= \omega_i, \\ \dot{\omega}_i &= P_i - \alpha_i\omega_i - P_i^{\mathrm{el}}(\boldsymbol{\Theta}, \boldsymbol{E}), \\ \dot{E}_i &= E_i^f - E_i + X_i I_i(\boldsymbol{\Theta}, \boldsymbol{E}), \end{aligned} \tag{1}$$

where the dot denotes differentiation with respect to time t. Here $\boldsymbol{\Theta} \in \mathbb{R}^N$ denotes the vector of the power angles, $\boldsymbol{\omega} = \dot{\boldsymbol{\Theta}}$ the angular frequency, both regarding the grid reference frame (rotating at, e.g., $\Omega = 2\pi \times 50$ Hz in Europe), and $\boldsymbol{E} \in \mathbb{R}_+^N$ the vector of terminal voltage amplitudes. Here, $\mathbb{R}_+$ denotes the set of non-negative real numbers such that each component $E_i \geq 0$. The remaining machine parameters are the power input or output $P_i \in \mathbb{R}$ (negative for consumers and positive for generators), the mechanical damping $\alpha_i > 0$, the voltage set point $E_i^f > 0$, and the reactance $X_i \geq 0$ of the synchronous machine i. The coupling functions $P_i^{\mathrm{el}} : \mathbb{R}^N \times \mathbb{R}^N \to \mathbb{R}$ and $I_i : \mathbb{R}^N \times \mathbb{R}^N \to \mathbb{R}$ represent, respectively, the electrical powers and the currents exchanged between the N synchronous machines through the transmission lines. A transmission line connecting nodes i and j is modeled by a series admittance $y_{ij} = g_{ij} + \imath b_{ij} \in \mathbb{C}$, with a conductance $g_{ij} = g_{ji} > 0$ and inductive susceptance $b_{ij} = b_{ji} < 0$, as well as a parallel susceptance, also called shunt susceptance $\gamma_{ij} > 0$ modeling capacitive effects arising between the transmission line and its surroundings. In general, all three quantities scale with the length of the transmission line. While conductance g_{ij} and susceptance magnitude $|b_{ij}|$ decrease proportional to line length, the shunt susceptance increases roughly proportionally to line length.[17] For long transmission lines of several hundred kilometers, one has to consider the line parameters to be distributed across the line length. According to Ref. 17, for overhead transmission lines up to approximately $\ell_0 = 240\,\mathrm{km}$, a lumped equivalent circuit model is assumed (also known as a Π-equivalent circuit), where the series line elements y_{ij} are concentrated at the center of the transmission line and the half of the shunts $\gamma_{ij}/2 = \Gamma_i = \Gamma_j$ are concentrated on both ends of the transmission line. For shorter transmission lines, below about $\ell_0 = 80\,\mathrm{km}$, shunts are negligible, i.e., small compared to $|b_{ij}|$ and $\Gamma_i = \Gamma_j \to 0$ as $\ell_0 \to 0$. If nodes i and j are not connected, all parameters $g_{ij} = b_{ij} = \Gamma_i = \Gamma_j = 0$. Lossless transmission, i.e., neglecting Ohmic losses ($g_{ij} = 0$) is taken as a reasonable idealization in high voltage power grid modeling,[2] such that transmitted powers and currents read[2,9]

$$\begin{aligned} P_i^{\mathrm{el}}(\boldsymbol{\Theta}, \boldsymbol{E}) &= \sum_{j=1}^{N} B_{ij} E_i E_j \sin(\Theta_i - \Theta_j), \\ I_i(\boldsymbol{\Theta}, \boldsymbol{E}) &= \sum_{j=1}^{N} B_{ij} E_j \cos(\Theta_j - \Theta_i). \end{aligned} \tag{2}$$

Here, symmetric susceptances ($B_{ij} = B_{ji} = -b_{ij} \geq 0$)[2] constitute a symmetric susceptance matrix $B = B^{\mathsf{T}} \in \mathbb{R}^{N\times N}$, with the diagonal elements $B_{ii} < 0$ being self-susceptances. Kirchhoff's nodal law requires that the self-susceptances are the negative sum over all off-diagonal elements in the same row, plus the shunt susceptances at the node, yielding

$$B_{ii} = \Gamma_i - \sum_{j=1, j\neq i}^{N} B_{ij} < 0. \tag{3}$$

First, we consider the parameters Γ_i as free model parameters and study their implications on the system's stability. Later, we will discuss the physically relevant magnitude of Γ_i. The system equation (1) with substituted coupling function equation (2) reads

$$\dot{\Theta}_i = \omega_i, \tag{4a}$$

$$\dot{\omega}_i = P_i - \alpha_i\omega_i + \sum_{j=1}^{N} B_{ij}E_iE_j \sin(\Theta_j - \Theta_i), \tag{4b}$$

$$\dot{E}_i = E_i^f + (X_i\Gamma_i - 1)E_i + X_i \sum_{j=1, j\neq i}^{N} B_{ij}(E_j\cos(\Theta_j - \Theta_i) - E_i). \tag{4c}$$

Power grids are operated near a fixed point state, which for the third-order model is a fixed point

$$(\boldsymbol{\Theta}^*, \boldsymbol{\omega}^*, \boldsymbol{E}^*), \tag{5}$$

given by a simultaneous solution to Eqs. (4a)–(4c) at zero rates of change,

$$\dot{\Theta}_i = \dot{\omega}_i = \dot{E}_i = 0 \quad \text{for all } i \in \{1, 2, \dots, N\}. \tag{6}$$

The existence of fixed points depends on the specific choices of the nodal parameters E_i^f, P_i, X_i, the line susceptances B_{ij} and Γ_i. For instance, a fixed point only exist if the powers P_i are in balance,

$$0 = \sum_{i=1}^{N} P_i. \tag{7}$$

Furthermore, from the paradigmatic Kuramoto model,[18] it is well known that the coupling strengths have to be sufficiently large to compensate the powers P_i to allow the system to settle into a fixed point. Since for the third-order model (4c) the fixed point coupling strengths

$$K_{ij} := B_{ij}E_i^*E_j^* \tag{8}$$

are bound by

$$K_{ij} \le B_{ij}\left(\frac{E_l^f}{1 - X_l\Gamma_l} + X_l\mu\right)^2 \le B_{ij}\left(\frac{E_l^f}{1 - X_l\Gamma_l}\right)^2, \tag{9}$$

with the index l denoting the largest of the fixed point voltage amplitude $E_l^* \ge E_i^*$ for all $i \in \{1, 2, \dots, N\}$ and $\mu \le 0$, we conclude that E_i^f and susceptances B_{ij} with $i \neq j$ have to be sufficiently large. Furthermore, the reactances X_i have to be sufficiently small. We derive necessary conditions for the existence of a fixed point in the Appendix.

Fixed voltages E_i^* and fixed frequencies ω_i^* are desired in power grid operations, as well as that the system relaxes back to the fixed point when exposed to small perturbations.

Whether the system relaxes back toward the fixed point is characterized by the linear stability of the corresponding fixed point of the system.[19] At a fixed point $(\boldsymbol{\Theta}^*, \boldsymbol{0}, \boldsymbol{E}^*)$, the evolution of the linear response $(\boldsymbol{\vartheta}, \boldsymbol{\nu}, \boldsymbol{\epsilon})$ of the system [(4a)–(4c)] is governed by

$$\begin{pmatrix} \dot{\boldsymbol{\vartheta}} \\ \dot{\boldsymbol{\nu}} \\ \dot{\boldsymbol{\epsilon}} \end{pmatrix} = \begin{pmatrix} 0 & I_N & 0 \\ \Lambda & -\alpha I_N & A \\ A^\top & 0 & C \end{pmatrix} \begin{pmatrix} \boldsymbol{\vartheta} \\ \boldsymbol{\nu} \\ \boldsymbol{\epsilon} \end{pmatrix} =: J \begin{pmatrix} \boldsymbol{\vartheta} \\ \boldsymbol{\nu} \\ \boldsymbol{\epsilon} \end{pmatrix}, \tag{10}$$

where $I_N \in \mathbb{R}^{N\times N}$ denotes an identity matrix and $\Lambda, A, C \in \mathbb{R}^{N\times N}$ are submatrices of the Jacobian matrix $\boldsymbol{J}$. The submatrices are defined via their matrix elements,

$$\Lambda_{ij} = \begin{cases} B_{ij}E_i^*E_j^*\cos(\Theta_j^* - \Theta_i^*) & \text{for } i \neq j, \\ -\sum_{k\neq i} B_{ik}E_i^*E_k^*\cos(\Theta_k^* - \Theta_i^*) & \text{for } i = j, \end{cases}$$

$$A_{ij} = \begin{cases} B_{ij}E_i^*\sin(\Theta_j^* - \Theta_i^*) & \text{for } i \neq j, \\ \sum_k B_{ik}E_k^*\sin(\Theta_k^* - \Theta_i^*) & \text{for } i = j, \end{cases} \tag{11}$$

$$C_{ij} = \begin{cases} X_iB_{ij}\cos(\Theta_j^* - \Theta_i^*) & \text{for } i \neq j, \\ X_i\Gamma_i - 1 - X_i\sum_{k\neq i} B_{ik} & \text{for } i = j. \end{cases}$$

The matrix J has one eigenvalue $\lambda_0 = 0$ corresponding to the eigenvector $\boldsymbol{v}_0 = (\boldsymbol{1}, \boldsymbol{0}, \boldsymbol{0})^\top$, indicating that the system is marginally stable along $\boldsymbol{v}_0$.[6,8,9] Nevertheless, since a shift along $\boldsymbol{v}_0$ does not change the physical state of the system, we, thus, only consider the system's linear stability in the orthogonal space[6]

$$\mathcal{D}^\perp = \left\{\boldsymbol{x} \in \mathbb{R}^{3N} | \boldsymbol{x}\boldsymbol{v_0} = 0\right\}. \tag{12}$$

As shown by Sharafutdinov *et al.* (Proposition 1 in Ref. 6), the asymptotic stability of the system in $\mathcal{D}^\perp$ (a negative definite J) implies that both submatrices Λ, the rotor angle subsystem, and C, the voltage subsystem, are negative definite themselves, i.e.,

$$J \text{ is negative definite} \Rightarrow \Lambda \text{ and } C \text{ are negative definite.} \tag{13}$$

Moreover, the proposition gives more restrictive conditions on the interplay between both subsystems that we do not mention here as they have no implication on the further analysis in this work. In this way, three routes to instability in the third-order model of synchronous machines are established:[6] one pure rotor angle instability, where Λ loses negative definiteness; one pure voltage instability, where C loses negative definiteness; and a third route resulting from an interplay between both subsystems, where a fixed point for both voltage and rotor angle equation cannot be determined simultaneously.

In particular, if the real parts of any eigenvalue of either one of the two submatrices C or Λ crosses zero from below (excluding $\lambda_0 = 0$ for Λ), the entire systems' fixed point becomes linearly unstable. Related earlier work has shown that one condition for Λ to be negative definite is[2,20]

$$|\Theta_j - \Theta_i| \le \frac{\pi}{2} \tag{14}$$

for all adjacent synchronous machines i and j, i.e., those directly connected by a transmission line. We now focus on the analysis of the voltage subsystem characterized by the matrix C by applying the Gershgorin disk theorem.[21] The broadly applicable theorem states[21–25] that for any square matrix $M \in \mathbb{C}^{N\times N}$ all the eigenvalues λ_j^M for all $j \in \{1, 2, \ldots, N\}$ are in the union

$$\lambda_j^M \in \bigcup_{i=1}^{N} \mathcal{G}_i \tag{15}$$

of N disks

$$\mathcal{G}_i := \left\{ z \in \mathbb{C} \;\middle|\; |z - M_{ii}| \le \sum_{j\neq i} |M_{ij}| \right\}. \tag{16}$$

The diagonal elements M_{ii} define the center of the disk, while the sum across the absolute values of the off-diagonal elements of the same row defines its radius. Since linear stability of the voltage subsystem alone is ensured if all eigenvalues λ_i^C of the matrix C have a negative real part, we evaluate under which conditions all the Gershgorin disks are entirely on the left-hand side of the imaginary axis.

To this end, we define the directed margin d_i

$$d_i := \sup \left\{ \mathrm{Re}(q) \mid q \in \mathcal{G}_i \right\} \tag{17}$$

between the imaginary axis and the Gershgorin disk (see Fig. 1). A negative margin for all i ensures linear stability of the voltage subsystem characterized by C. Thus, for parameters where all $d_i < 0$, voltage instabilities do not occur. For general setups of the network and machine parameters, the margins d_i of symmetric matrix C satisfy

$$\begin{aligned} d_i &= C_{ii} + \sum_{j\neq i}^{N} |C_{ij}| \\ &= -1 + X_i\Gamma_i - X_i \sum_{j=1, j\neq i}^{N} B_{ij} \\ &\quad + X_i \sum_{j=1, j\neq i}^{N} |B_{ij} \cos(\Theta_j^* - \Theta_i^*)| \\ &= -1 + X_i\Gamma_i + X_i \sum_{j\neq i}^{N} B_{ij}(|\cos(\Theta_j^* - \Theta_i^*)| - 1) \\ &\le -1 + X_i\Gamma_i. \end{aligned} \tag{18}$$

In the first step, we apply the definition of the Gershgorin disk $\mathcal{G}_i$ to matrix $M = C$. In the second step, we substitute matrix elements of C according to Eq. (11), exploiting that $X_i > 0$. In the third step, as $B_{ij} > 0$ for $i \neq j$, we factor it out and regroup the terms. Finally, bounding the cosine function by its upper bound $1 = \max\{\cos(x) \mid x \in \mathbb{R}\}$ provides an upper bound for d_i. We set the upper bound $X_i\Gamma_i - 1 = 0$ of d_i and obtain

$$X_{\mathrm{crit}}(\Gamma) = \frac{1}{\Gamma}, \tag{19}$$

a lower bound for the critical parameter X_{crit} with $\Gamma = \max\{\Gamma_i \mid i \in \{1, 2, \ldots, N\}\}$. For all $0 \le X \le X_{\mathrm{crit}}(\Gamma)$ the matrix C is negative definite as shown via the Gershgorin disk theorem. For $X > X_{\mathrm{crit}}$, the matrix may have positive eigenvalues $\lambda_i^C > 0$ but due to the upper bound approximation in Eq. (18) and this is not guaranteed and, hence, referred to as potentially unstable region in Fig. 2. For our further analysis, we will rely on the stable regime and do not need further knowledge about the potentially unstable region. We have derived a bound $X_{\mathrm{crit}}(\Gamma)$, for which

$$\begin{aligned} X < X_{\mathrm{crit}}(\Gamma) &\iff \text{voltage stability}, \\ X \ge X_{\mathrm{crit}}(\Gamma) &\iff \text{potential voltage instability} \end{aligned} \tag{20}$$

holds. Our result shows that under the assumption of weakly diagonally dominance[26] of the admittance matrix $Y = G + \imath B$, i.e., $\Gamma_i \le 0$, the system exhibits no voltage instability neither for finite nor infinite voltage amplitudes.

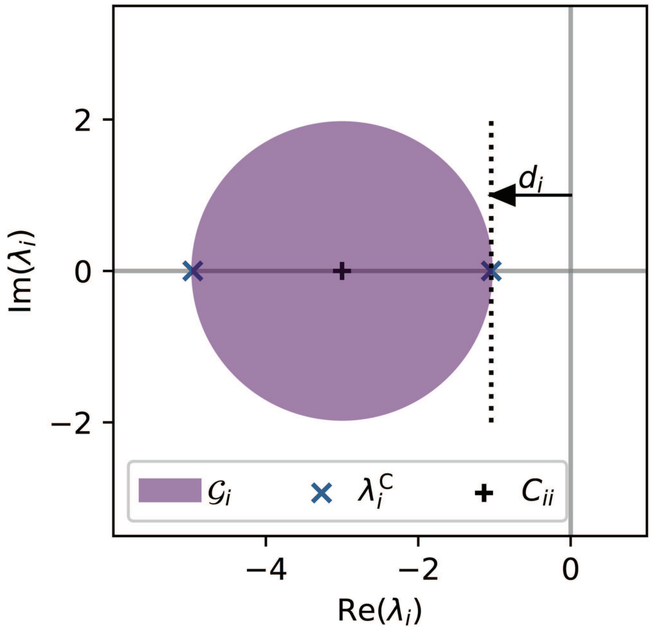

FIG. 1. Negative margins d_i ensure linear stability of the voltage subsystem: The voltage subsystem of $N = 2$ coupled third-order synchronous machines is evaluated in terms of the margin d_i. The two Gershgorin disks coincide, and the true positions of the eigenvalues are precisely on the borders of the disks. The parameters are $P_1 = -P_2 = 1.5$, $B_{12} = B_{21} = 2$, $E^f = 2$, 1.0, and $\Gamma_1 = \Gamma_2 = 0$.

III. ABSENCE OF PURE VOLTAGE INSTABILITIES FOR $N = 2$

The above analysis proves for $X_i \le X_{\mathrm{crit}}(\Gamma)$ the linear stability of the voltage subsystem. However, it does not take into account whether fixed points exist in the potentially unstable region at all. Hence, we do not know at this point whether a transition to an unstable voltage subsystem at all is possible or not. For instance, in the simplest system of $N = 2$ coupled third-order synchronous machines, one can show that all fixed points are found in the stable region of the voltage subsystem for arbitrary choices of Γ. The fixed point of this system configuration is explicitly given via the set of

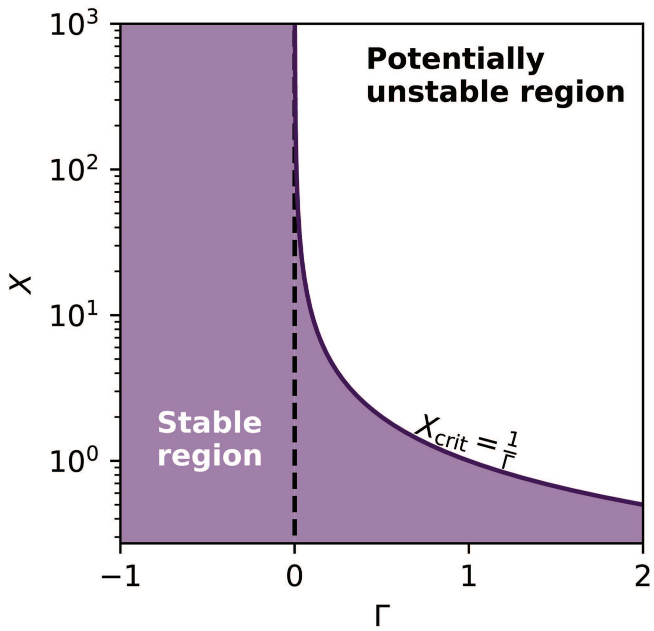

FIG. 2. The minimal stable region of the voltage subsystem depends on the parameter Γ: the matrix of the voltage subsystem is negative definite in the purple region such that no pure voltage instability occurs here. In particular, for $\Gamma \leq 0$, the voltage subsystem alone is linearly stable for all $X \in \mathbb{R}^+$. This analysis holds for arbitrary system sizes N, parameter settings, and, thus, network topologies.

equations,

$$\begin{aligned}
0 &= \omega_1^*,\\
0 &= \omega_2^*,\\
0 &= P_1 - \alpha_1\omega_1^* + B_{12}E_1^*E_2^* \sin(\Theta_2^* - \Theta_1^*),\\
0 &= P_2 - \alpha_2\omega_2^* + B_{12}E_1^*E_2^* \sin(\Theta_1^* - \Theta_2^*),\\
0 &= E^f - E_1^* + X\Gamma E_1^* + XB_{12}(E_2^* \cos(\Theta_2^* - \Theta_1^*) - E_1^*),\\
0 &= E^f - E_2^* + X\Gamma E_2^* + XB_{12}(E_1^* \cos(\Theta_2^* - \Theta_1) - E_2^*),
\end{aligned} \tag{21}$$

which effectively reduces to

$$0 = P + B_{12}E^*E^* \sin(\Delta\Theta^*), \tag{22a}$$

$$0 = E^f - E^* + X\Gamma E^* + XB_{12}(E^* \cos(\Delta\Theta^*) - E^*), \tag{22b}$$

with $E_1 = E_2 = E^*$ (which follows from subtracting the voltage equations from one another) and $\Delta\Theta^* = \Theta_2^* - \Theta_1^*$. In this configuration, C reads

$$C = \begin{pmatrix} -X(B_{12} - \Gamma) - 1 & XB_{12}\cos(\Delta\Theta), \\ XB_{12}\cos(\Delta\Theta) & -X(B_{12} - \Gamma) - 1 \end{pmatrix} \tag{23}$$

and has the two real eigenvalues

$$\lambda_\pm^C = -X(B_{12} - \Gamma) - 1 \pm XB_{12}\cos(\Delta\Theta). \tag{24}$$

To investigate where the voltage subsystem changes its linear stability, we analyze the system, rearranging Eq. (24) for its largest eigenvalue via Eq. (24) λ_+^C such that

$$XB_{12}\cos(\Delta\Theta) = X(B_{12} - \Gamma) + 1 + \lambda_+^C. \tag{25}$$

We substitute the latter into Eq. (22b) and find

$$\begin{aligned}
0 &= E^f - E^* + X\Gamma E^* + E^*(XB_{12} - X\Gamma + 1) - XB_{12}E^* + \lambda_+^C E^*,\\
0 &= E^f + \lambda_+^C E^*.\\
&\Rightarrow E^* = -\frac{E^f}{\lambda_+^C}.
\end{aligned} \tag{26}$$

Given that $E^f > 0$ is a strictly positive machine parameter, we conclude that for $N = 2$, a transition from λ_+^C¡0 (stable) to $\lambda_+^C > 0$ (unstable operating point) requires a passing of E^* through infinity; moreover, $\lambda_+^C > 0$ requires a non-physical negative voltage amplitude $E^* < 0$, under any configuration of all parameters of the model system. The $N = 2$ model system, therefore, shows no physically meaningful transition to a linear unstable voltage subsystem, i.e., no pure voltage instability. Instead of observing a transition from a linearly stable fixed point to a linearly unstable fixed point, we instead observe the loss of a physical meaningful fixed point. For short transmission line lengths $\ell_0 \leq 80$ km, the shunt susceptances are negligible,[17] with $\Gamma_i \to 0$ as $\ell_0 \to 0$, which results in $X_{crit}(\Gamma) \to \infty$ (see Fig. 2). The X_i constitute finite and positive machine parameters such that for general system sizes $N \geq 2$ with transmission line lengths up to $\ell_0 = 80$ km, the voltage subsystem is always linearly stable. In Sec. IV, we extend this observation to transmission line lengths up to $\ell_0 = 240$ km by first considering real-world parameters, showing that real-world systems are generally far away from the critical reactance X_{crit} (see Fig. 2), and a general mathematical analysis under the condition of finite and positive voltage amplitudes E_i^* in the voltage subsystem is always linearly stable.

IV. ABSENCE OF PURE VOLTAGE INSTABILITIES $N > 2$

Typical series line resistance and reactances, as well as parallel shunt reactances, are available in the existing literature. Here, we consider averaged values of Γ_i and b_{ij} for 18 different overhead transmission lines available in Hernandez *et al.*[17,27] (Table 13.13a), for which the average susceptance is given by $\langle b_{ij}\rangle\ell_0 \approx -3\,\Omega^{-1}$ km, while the shunt susceptance per kilometer is given by $\langle\Gamma_i\rangle/\ell_0 \approx 2.5 \times 10^{-6} (\Omega\,\text{km})^{-1}$ at a frequency of 60 Hz. The shunt susceptance is increasing with line length, while the series susceptance is decreasing in magnitude with line length. For a length $\ell_0 = 80$ km, we find that Γ_i is in the order of 0.5% compared to the magnitude of the series susceptance, while for 240 km, it is of the order of 5%. The critical reactance X_{crit} in Eq. (19) is given by the inverse of the shunt susceptance Γ_i. In other words, to allow the system to potentially show positive eigenvalues λ^C of the matrix C, one would require that the absolute shunt reactance $|1/\Gamma_i|$ of the transmission system is equal to the reactance X_i of the stator winding of the synchronous machine. For a transmission line of $\ell_0 = 240$ km, reactance X_i of the stator winding would need to exceed 1600 Ω, while real-world parameters (example of an 555 MW synchronous generator)[26] are in the range of up to 0.3 Ω, way afar from the critical reactance.

Moreover, we show that even in the case of the reactance $X_i \to X_{crit}$, the fixed point voltage E_i^* of at least one machine has to approach infinity as $\Gamma_i X_i \to 1$; thus, $X_i \to X_{\rm crit}$. Inspecting the voltage fixed point equation (4c) for the largest fixed point voltage amplitude $E_i^* \geq E_j^*$ for all $j \in \{1, 2, \ldots, N\}$ yields [see Appendix Eq. (A10)]

$$E_i^* \geq \frac{E^f}{1 - X_i \Gamma_i} \quad \text{for } \Gamma_i X_i < 1, \tag{27}$$

from which we conclude that $E_i^* \to \infty$ for $X_i \Gamma_i \to 1$ from below, thus $X_i \to X_{\rm crit}$ as defined in Eq. (19). Moreover, for $X_i \Gamma_i > 1$, we find

$$E_i^* \leq \frac{E^f}{1 - X_i \Gamma_i} \quad \text{for } \Gamma_i X_i > 1, \tag{28}$$

thus E_i^* being negative, which constitutes a nonphysical solution for an amplitude. Even worse, as $E_i^* \geq E_j^*$ all fixed point voltage amplitudes have to be negative in the potentially unstable voltage subsystem regime. We conclude that the theoretically existing fixed point solutions with a positive eigenvalue λ^C of the matrix C are thus non-physical and do not represent the physical reality in the world's power grids.

V. VOLTAGE COLLAPSE IN THIRD-ORDER SYNCHRONOUS MACHINE DYNAMICS

Despite the fact that the physical third-order model of synchronous machines does not exhibit pure voltage instabilities, i.e., linearly unstable voltage subsystems, we emphasize that it still captures the known phenomenon of voltage collapse, i.e., substantial voltage changes upon parameter changes[2,3,26,28] Voltage collapse has been discussed as one of the root causes of various real-world power outages.[2,3] In this section, we illustrate numerically that the third-order model of synchronous machines has the capability to undergo voltage collapse. The underlying cause, instead of a linear instability of the voltage subsystem, is a saddle-node bifurcation at which the existence of two fixed points is lost, including the stable one. The saddle-node bifurcation occurs when transmission line capacities at the respective voltage levels are not sufficient to meet the power demand P of the consumer. We investigate this (see Fig. 3) for a simple system of $N = 2$ nodes and one transmission line, as in Sec. II.

Figure 3 displays the loss of existence of two fixed points upon parameter changes of the active power P and a possible way of restoring higher voltage levels. Beyond the critical value of the power $P_{\rm max} = B_{12}(E^*)^2$ [see Eq. (22a)], where $P_{\rm max}$ has to compensate for the power P that needs to be transported across a transmission line, the stable fixed point is lost, and the third-order dynamics causes the voltage amplitudes to drop significantly. The third-order model, thus, captures the phenomenon of voltage collapse. However, the root cause is not the loss of the stability of the voltage subsystem but a power overload of the transmission line and the related loss of fixed points. Even at P below the previously valid critical value of the power $P_{\rm max}$, the system does *not* relax back to the stable fixed point. Significantly smaller power values $P < B_{12}(E(t))^2$ are needed to stabilize the power transmission. See Fig. 3 for details of the example.

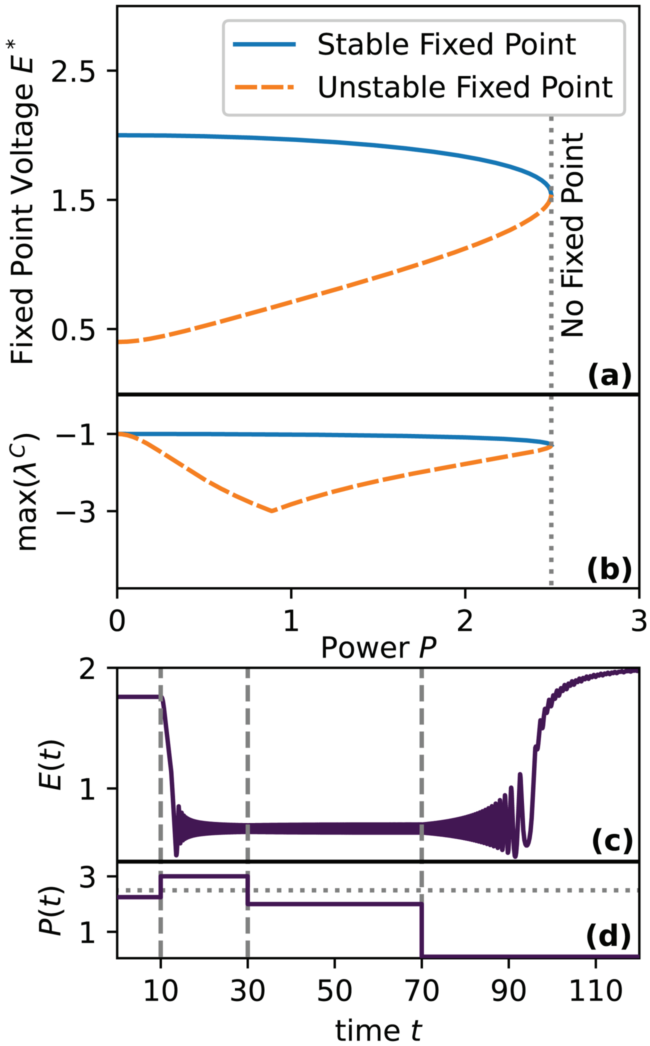

FIG. 3. Voltage collapse without pure voltage instability. (a) Fixed point voltage amplitude E^* changes with the active power P in a $N = 2$ node system. The system exhibits two relatively large voltage fixed points, one stable (solid line) and one unstable (dashed line) that annihilate in a saddle-node bifurcation (near $P = 2.5$), beyond which no real solution for Eqs. (22a) and (22b) exists. (b) Consistently negative eigenvalues indicate that the voltage subsystem is linearly stable for the whole range of P and the stable and unstable branch of the entire third-order dynamics where the fixed point exists. (c) and (d) Time evolution of the voltage amplitude $E(t)$ upon temporally changing power $P(t)$. At $t = 10$, the power demand P increases (instantaneously) from 2.25 to 3, at $t = 30$ the power demand P is lowered to 2 and again at $t = 70$ to $P = 0.1$. Network parameters are $\Gamma_1 = \Gamma_2 = 0$, $B_{12} = B_{21} = 2$, $X = 1.0$, $\alpha = 0.1$, and $E^f = 2$.

VI. CONCLUSION

Interestingly, real-world power outages have indeed been tied to effects described as voltage instabilities. However, this terminology referred to voltage drops,[1,2] which we have observed numerically in the third-order model upon changes of parameters without changes in the stability of any operating state. The power overload of transmission lines is the root cause of the voltage collapse. We, thus, emphasize that the term "voltage collapse" is to be carefully separated from the term "voltage instability," which relies on the linear stability of the voltage subsystem. These two phenomena are mathematically not connected. Another class of power system models, given by algebraic differential equations, was studied extensively in the literature[4,5] in terms of voltage collapse. The fundamental difference of that model class is that consumers are assumed to have fixed power angles, Θ, as well as fixed active and active power demand. Thus, they represent algebraic constraints to the dynamics of the generators. In such a setup, linearly stable, low voltage fixed points may be identified. It is particularly difficult to operate a system that is trapped at such a fixed point and bring it back to a high voltage fixed point.[4,5] A detailed analysis of a three bus system is given in Ref. 29. In contrast to the third-order model of power grids, these extended models exhibit changes of local stability properties upon parameter changes.

For the third-order model, it is sufficient to ensure that line capacity constraints are satisfied to ensure stable, high voltage operation. Given the results presented above, two research paths open up to further study voltage stability properties in power system models. First, one could factor in Ohmic losses, i.e., $G_{ij} > 0$, and analyze whether local stability properties of the voltage subsystem undergo a bifurcation. Second, one could investigate non-local stability properties in the third-order model by numerically analyzing basin stability[30,31] for voltage and rotor angle perturbations. The basin size may depend strongly on the line load. Furthermore, it would be of interest to extend the basin stability argument to the model of differential algebraic equations.[4,5]

ACKNOWLEDGMENTS

We thank Malte Schröder and Philip Marszal for valuable comments on the manuscript. We gratefully acknowledge support from the Bundesministerium für Bildung und Forschung (BMBF, Federal Ministry of Education and Research) under Grant No. 03EK3055F.

AUTHOR DECLARATIONS

Conflict of Interest

The authors have no conflicts to disclose.

DATA AVAILABILITY

The data that support the findings of this study are available within the article.

APPENDIX: NECESSARY CONDITIONS FOR THE EXISTENCE OF FIXED POINT

Here, we motivate our statement in the main text about parameter configurations under which fixed points of Eq. (4a)–(4c), i.e., points where $\dot{\Theta}_i = \dot{\omega}_i = \dot{E}_i = 0$ for all i exist.

Corollary A.1. *The powers P_i across the network of third-order synchronous machines have to be in balance*

$$0 = \sum_{i=1}^{N} P_i \tag{A1}$$

to allow the entire system to settle to a fixed point.

Proof. To show that such balance is a necessary condition for the existence of a fixed point, we take the sum over all N nodes[2,6] of the rotor angle equation (4b), yielding

$$0 = \sum_{i=1}^{N} (P_i - \alpha_i \omega_i^*) + \sum_{i=1}^{N} \sum_{j=1}^{N} B_{ij} E_i^* E_j^* \sin(\Theta_j^* - \Theta_i^*). \tag{A2}$$

The sine functions are antisymmetric, while B is symmetric against an exchange of indices such that the double sum equals zero. Furthermore, Eq. (4a) implies that $\omega_i^* = 0$ for all i and, therefore,

$$0 = \sum_{i=1}^{N} P_i. \tag{A3}$$

□

The second assertion is that the voltage set points E_i^f have to be sufficiently large for a fixed point to exist. We identify the effective coupling strengths K_{ij} in Eq. (4b),

$$K_{ij} = B_{ij} E_i^* E_j^*. \tag{A4}$$

From the paradigmatic Kuramoto model,[18] it is known that the coupling strength needs to be sufficiently large in order to compensate the parameters P_i for all i to allow the system to settle in a phase-locked state. Due to the first condition, Eq. (A1) a phase-locked state is also a fixed point.

Corollary A.2. *The fixed point coupling strength $K_{ij} = B_{ij} E_i^* E_j^*$ of the rotor angle dynamics is bound by*

$$K_{ij} \le B_{ij} \left(\frac{E^f}{1 - X_i \Gamma_i} + X_i \mu \right)^2 \le B_{ij} \left(\frac{E^f}{1 - X_i \Gamma_i} \right)^2, \tag{A5}$$

with $\mu \le 0$ for networks of N third-order synchronous machines with $E_i^f = E^f$ for all $i \in \{1, 2, \dots, N\}$.

Proof. We prove that relation equation (A5) holds for every synchronous machine individually. We assume that a fixed point of the entire system $\boldsymbol{\Theta}^* \in \mathbb{R}^N, \boldsymbol{E}^* \in \mathbb{R}^N$ exists. We exploit the following properties:

$$\begin{gathered} E_i^f = E^f > 0, \\ E_i^* > 0, \\ X_i > 0, \\ B_{ij} \ge 0, \\ \Gamma_i \ge 0, \\ \cos(x) \le 1 \text{ for all } x \in \mathbb{R} \end{gathered} \tag{A6}$$

for all $i \in \{1, 2, \dots, N\}$. Among the finite number of fixed point voltage amplitudes, E_i^* we pick the largest E_i^* such that for all $j \neq i$

$$E_i^* \ge E_j^* \tag{A7}$$

holds. For the synchronous machine i, the voltage amplitude fixed point defining equations reads

$$0 = E^f + (X_i\Gamma_i - 1)E_i^* + X_i \sum_{j=1, j\neq i}^{N} B_{ij}(E_j^* \cos(\Theta_j^* - \Theta_i^*) - E_i^*). \tag{A8}$$

We exploit that B_{ij}, E_j^*, X_i are non-negative, as well as the upper bound of $\cos(x)$ to evaluate

$$\begin{aligned} 0 &\leq E^f + (X_i\Gamma_i - 1)E_i^* + X_i \sum_{j=1, j\neq i}^{N} B_{ij}(E_j^* - E_i^*) \\ &= E^f + (X_i\Gamma_i - 1)E_i^* + X_i\mu, \end{aligned} \tag{A9}$$

with $\mu \leq 0$ because we have chosen the largest voltage amplitude E_i^*. We conclude

$$\begin{aligned} 0 &\leq E^f + (X_i\Gamma_i - 1)E_i^* + X_i\mu \\ &\leq E^f + (X_i\Gamma_i - 1)E_i^* \\ &\Rightarrow E_i^* > \frac{E^f}{1 - X_i\Gamma_i}. \end{aligned} \tag{A10}$$

Lacking shunts, i.e., $\Gamma_i = 0$, the latter is equivalent to

$$E_i^* \leq E^f, \tag{A11}$$

and as $E_i^* \geq E_j^*$ for all $j \in \{1, 2, \ldots, N\}$, we have shown that relation equation (A11) holds for all $i \in \{1, 2, \ldots, N\}$ without shunts and Eq. (A10) holds in the presence of shunts. The coupling strength K_{ij} is bounded by

$$K_{ij} = B_{ij}E_i^*E_j^* \leq B_{ij}\left(\frac{E^f}{1 - X_i\Gamma_i}\right)^2. \tag{A12}$$

From this, we conclude that parameter E^f has to be set sufficiently large to provide sufficient coupling strength for the system to settle into a fixed point. □

REFERENCES

[1] A. Casavola, D. Famularo, G. Franzè, and M. Sorbara, "Set-points reconfiguration in networked dynamical systems," in *Fault Detection, Supervision and Safety of Technical Processes 2006* (Elsevier, 2007), pp. 132–137.
[2] J. Machowski, J. W. Bialek, and J. Bumby, *Power System Dynamics: Stability and Control* (Wiley, 2011), ISBN: 9781119965053.
[3] J. W. Simpson-Porco, F. Dörfler, and F. Bullo, "Voltage collapse in complex power grids," Nat. Commun. **7**(1), 10790 (2016).
[4] S. Ayasun, C. O. Nwankpa, and H. G. Kwatny, "Computation of singular and singularity induced bifurcation points of differential-algebraic power system model," IEEE Trans. Circuits Syst. I: Reg. Papers **51**(8), 1525–1538 (2004).
[5] H. Kwatny, A. Pasrija, and L. Bahar, "Static bifurcations in electric power networks: Loss of steady-state stability and voltage collapse," IEEE Trans. Circuits Syst. **33**(10), 981–991 (1986).
[6] K. Sharafutdinov, L. R. Gorjão, M. Matthiae, T. Faulwasser, and D. Witthaut, "Rotor-angle versus voltage instability in the third-order model for synchronous generators," Chaos **28**(3), 033117 (2018).
[7] G. Filatrella, A. H. Nielsen, and N. F. Pedersen, "Analysis of a power grid using a Kuramoto-like model," Eur. Phys. J. B **61**(4), 485–491 (2008).
[8] M. Rohden, A. Sorge, M. Timme, and D. Witthaut, "Self-organized synchronization in decentralized power grids," Phys. Rev. Lett. **109**(6), 064101 (2012).
[9] K. Schmietendorf, J. Peinke, and O. Kamps, "The impact of turbulent renewable energy production on power grid stability and quality," Eur. Phys. J. B **90**(11), 222 (2017).
[10] B. Schäfer, C. Beck, K. Aihara, D. Witthaut, and M. Timme, "Non-Gaussian power grid frequency fluctuations characterized by Lévy-stable laws and superstatistics," Nat. Energy **3**(2), 119–126 (2018).
[11] M. Anvari, G. Lohmann, M. Wächter, P. Milan, E. Lorenz, D. Heinemann, M. Reza Rahimi Tabar, and J. Peinke, "Short term fluctuations of wind and solar power systems," New J. Phys. **18**(6), 063027 (2016).
[12] X. Zhang, S. Hallerberg, M. Matthiae, D. Witthaut, and M. Timme, "Fluctuation-induced distributed resonances in oscillatory networks," Sci. Adv. **5**(7), eaav1027 (2019).
[13] Y. Yang, T. Nishikawa, and A. E. Motter, "Small vulnerable sets determine large network cascades in power grids," Science **358**(6365), eaan3184 (2017).
[14] B. Schäfer, D. Witthaut, M. Timme, and V. Latora, "Dynamically induced cascading failures in power grids," Nat. Commun. **9**(1), 1975 (2018).
[15] D. Witthaut, F. Hellmann, J. Kurths, S. Kettemann, H. Meyer-Ortmanns and M. Timme, "Collective nonlinear dynamics and self-organization in decentralized powergrids," Rev. Mod. Phys. **94**, 015005 (2022).
[16] E. L. Owen, "The origins of 60-Hz as a power frequency," IEEE Ind. Appl. Mag. **3**(6), 8–14 (1997).
[17] M. Reta-Hernández, "Transmission line parameters," in *Electric Power Generation, Transmission, and Distribution: The Electric Power Engineering Handbook* (CRC Press, 2018), pp. 14-1–14-36.
[18] S. H. Strogatz, "From Kuramoto to Crawford: Exploring the onset of synchronization in populations of coupled oscillators," Physica D **143**(1–4), 1–20 (2000).
[19] S. H. Strogatz, *Nonlinear Dynamics and Chaos: With Applications to Physics, Biology, Chemistry and Engineering* (Westview Press, 2000).
[20] D. Manik, D. Witthaut, B. Schäfer, M. Matthiae, A. Sorge, M. Rohden, E. Katifori, and M. Timme, "Supply networks: Instabilities without overload," Eur. Phys. J. Spec. Top. **223**(12), 2527–2547 (2014).
[21] S. Gerschgorin, "Über die abgrenzung der eigenwerte einer matrix," Izvest. Akad. Nauk SSSR, Ser. Matemat. **7**(3), 749–754 (1931).
[22] J. Stoer and R. Bulirsch, *Numerische Mathematik* (Springer, 2002), Vol. 7.
[23] M. Timme, F. Wolf, and T. Geisel, "Topological speed limits to network synchronization," Phys. Rev. Lett. **92**(7), 074101 (2004).
[24] M. Timme and F. Wolf, "The simplest problem in the collective dynamics of neural networks: Is synchrony stable?," Nonlinearity **21**(7), 1579 (2008).
[25] R. W. Freund and R. W. Hoppe, *Stoer/Bulirsch: Numerische Mathematik 1* (Springer-Verlag, 2007).
[26] P. Kundur, *Power System Stability and Control* (McGraw-Hill Education, 1994), ISBN: 9780070359581.
[27] R. J. Lings, *EPRI AC Transmission Line Reference Book: 200 KV and Above*, 3rd ed. (Electric Power Research Institute, 2005).
[28] I. Dobson and H.-D. Chiang, "Towards a theory of voltage collapse in electric power systems," Syst. Control Lett. **13**(3), 253–262 (1989).
[29] R. E. Beardmore, "Double singularity-induced bifurcation points and singular Hopf bifurcations," Dyn. Stability Syst. **15**(4), 319–342 (2000).
[30] P. J. Menck, J. Heitzig, J. Kurths, and H. J. Schellnhuber, "How dead ends undermine power grid stability," Nat. Commun. **5**(1), 3969 (2014).
[31] A. Büttner, J. Kurths, and F. Hellmann, "Ambient forcing: Sampling local perturbations in constrained phase spaces" arXiv.2201.10909 (2022).